Spiral MRI Reconstruction Using Least Square Quantization Table

Dong Liang, Edmund Y. Lam, George S.K. Fung, and Xin Zhang

Department of Electrical and Electronic Engineering
The University of Hong Kong, Pokfulam Road, Hong Kong
{dliang,elam,skfung,xinzhang}@eee.hku.hk

Abstract. Recently, the authors introduced least square quantization table (LSQT) method to accelerate the direct Fourier transform to reconstruct magnetic resonance images acquired using a spiral trajectory. In this paper, we will discuss the LSQT further in its adaptability, reusability and choice of the number of groups. The experimental results show that the LSQT method has better adaptability for the different reconstruction cases than the equal phase line (EPL) and Kaiser-Bessel gridding methods. Additionally, it can be reused for reconstructing different images of varied sizes.

Keywords: Image reconstruction; spiral trajectory; least square quantization table; adaptability; reusability.

1 Introduction

Recently, non-Cartesian scanning in k-space, such as spiral, has received increased attention in Magnetic Resonance Imaging (MRI). However, when the data is acquired using a non-Cartesian k-space trajectory, image reconstruction can no longer be accomplished with a direct FFT. Therefore, the problem of reconstructing image from a set of nonuniformly sampled data has drawn more attention in the past few years. The Kaiser-Bessel griding is the most widely used method to solve this problem, where nonuniformly sampled data are first resampled onto a Cartesian grid and then a FFT is applied to reconstruct the image. As the most straightforward and accurate solution, the direct Fourier transform [1] has some advantages over other methods. Unfortunately, the high computational demand makes it impractical compared with methods that use the fast Fourier transform (FFT) [2]. Two algorithms, Equal-Phase-Line (EPL) and look-up table (LUT), were proposed to solve this problem [3,4]. The EPL method does not take into account the actual distribution of phases for each data, and therefore may cause a large quantization error and consequently a large reconstruction quality loss. Meanwhile, the LUT method is only efficient for small size images due to the huge memory required for storing a large size look-up table.

More recently, the authors introduced a new algorithm for accelerating the direct Fourier transform to reconstruct MR images acquired using a spiral trajectory. The algorithm, called least square quantization table (LSQT) [5,6], reduces

X. Gao et al. (Eds.): MIMI 2007, LNCS 4987, pp. 287–293, 2008.

the computation loads of direct Fourier transform with only a little quality loss. The results were shown to be more accurate than EPL and require less memory than LUT. In this paper, we will report further results in the LSQT method in terms of its adaptability, reusability and choice of the number of groups.

2 The Least Square Quantization Table Method

We summarize the LSQT method in this section. Further details can be found in [5]. When direct Fourier transform method is applied to reconstruct image I of size $N \times N$ from k-space data s with length L, the contribution of the pth data to the entire image space is [3] :

$$I_p(x, y) = s_p d_p \exp(j2\pi(xu_p + yv_p)). \tag{1}$$

where $x, y = [-N/2 : N/2 - 1]$ is image pixel and $u, v = [-1/2 : 1/2]$ is sampling position in k-space. d_p is the density compensation function. It can be seen from (1) that for a given $\{u_p, v_p\}$, if two pixels (x_1, y_1) and (x_2, y_2) have the same phase such that $2\pi(x_1u_p + y_1v_p) = 2\pi(x_2u_p + y_2v_p)$, the data s_p has the same contribution to the two pixel locations. Also, if we define $C_p = xu_p + yv_p$, because of the periodic property of the complex exponential function, C_p is also a periodic function with unity period and we can concentrate on the main phase band $[0, 2\pi)$, corresponding to the fractional part of C_p in $[0, 1)$, which we denoted as $\langle C_p \rangle$. If C_p is negative, we add an integer to it to bring it to between 0 and 1, and $\langle C_p \rangle$ then is the resulting fractional part. Thus, each pixel $\{x, y\}$ has a one-to-one correspondence to $\langle C_p \rangle$.

It is noted that if some pixels have the same $\langle C_p \rangle$, the acquired raw data in k-space have the same contribution to these pixels. Thus, all the pixels can be classified into groups, where each group is labeled by a different representative value and pixels in the same group receive the same contribution. If the contributions of the given data to all the groups are known, for a pixel, we only need to know which group it belongs to. Consequently, (1) is calculated only once for each group instead of for each pixel in the direct Fourier transform method. Therefore, the tradeoff between the reduction of computing loads and loss of image quality lies in the number of groups. Instead of requiring an exact value of $\langle C_p \rangle$ before two pixels can be classified into the same group, we use the Lloyd-Max quantization algorithm to classify all the pixels into only M groups where $M \ll N^2$. The group boundaries are calculated by quantizing the interval $[0, 1)$ into M bins in the least square sense of quantization error [7]. The representative value of each group is the centroid of the corresponding group, which is the optimal point to give the lowest quality loss.

Therefore, for the k-space data s with length L, we can pre-compute a least square quantization table (LSQT) $\mathcal{Q}$ of size $M \times L$. The construction of the table can be accomplished off-line and reused for the same k-space trajectory, being independent of the object being imaged. After loading the table, when a data arrives, the contributions of the data to all the groups can be calculated. Then for a pixel, we use binary-searching algorithm to map it to the corresponding

group and set contribution directly . Considering the symmetric and periodic properties of $\langle C_p \rangle$, only pixels where $x \geq 0$ need to undergo mapping [3].

3 Results on Adaptability and Reusability

Our experiments are performed with the Shepp and Logan mathematical phantom [8] with three different sizes, 64×64, 128×128 and 256×256. Spiral trajectory used in [5] was applied to generate k-space data from phantoms. The size of k-space data is 13,392. Then there are three cases of image reconstruction: $L > N \times N$, $L \approx N \times N$ and $L < N \times N$. M takes the values 16, 32, 64 and 128 as in [5].

Similar to that in [5], the reconstructed image obtained with the direct Fourier transform is used as a standard. The normalized Root Mean Square (nRMS) error is calculated after reconstructed images are scaled to a range of gray levels [0,255] and the Maximum Absolute Difference (MAD) is normalized by dividing by 255.

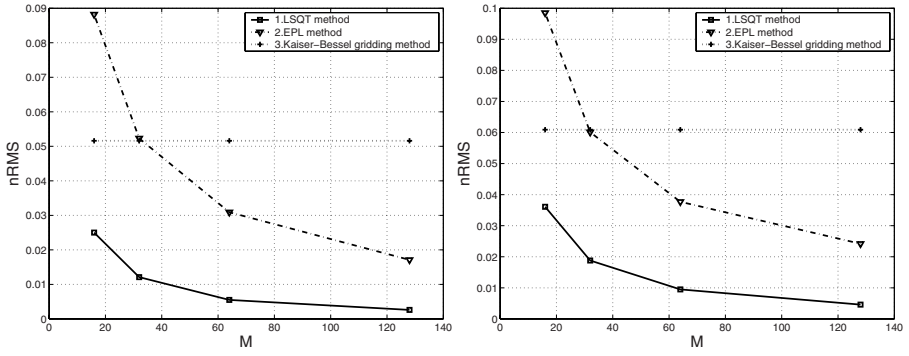

Fig. 1. (a) and (b) The nRMS of different methods against the number of groups for reconstructing N=64 and N=128 phantoms, respectively

Fig. 1 (a) and (b) shows the nRMS of different methods against the number of groups for reconstructing $N = 64$ and $N = 128$ phantoms, respectively. The performance of reconstructing $N = 256$ image from data acquired using this spiral trajectory can be found in [5]. For these cases, we can draw the same conclusion that the LSQT method can give more accurate reconstruction results than EPL and Kaiser-Bessel griding methods when M takes an appropriate value. Moreover, the LSQT method even when $M = 16$ performs better than the Kaiser-Bessel griding. The Kaiser-Bessel griding used here is the same as that used in [5].

Next we will explore the adaptability of different methods when facing different reconstructing cases, from oversampling to undersampling. Fig. 2 shows the

nRMS against the size of reconstructed phantoms for the LSQT, EPL and griding methods with different M, where the solid lines are for the LSQT, dashed lines for the EPL and dotted line for the Kaiser-Bessel griding. Theoretically, the nRMS error will become larger with increasing reconstructed image size while the number of k-space data is fixed, because the reconstruction case varies from $L > N \times N$ to $L < N \times N$. We can see from this figure that, the nRMS curves for the LSQT are flatter than those of EPL and Kaiser-Bessel griding methods with the same M in general. It means compared to other two methods, the LSQT has better adaptability for the different reconstruction cases. The reasons are because the actual distribution of $\langle C_p \rangle$ is taken into account and Lloyd-Max quantization algorithm is used.

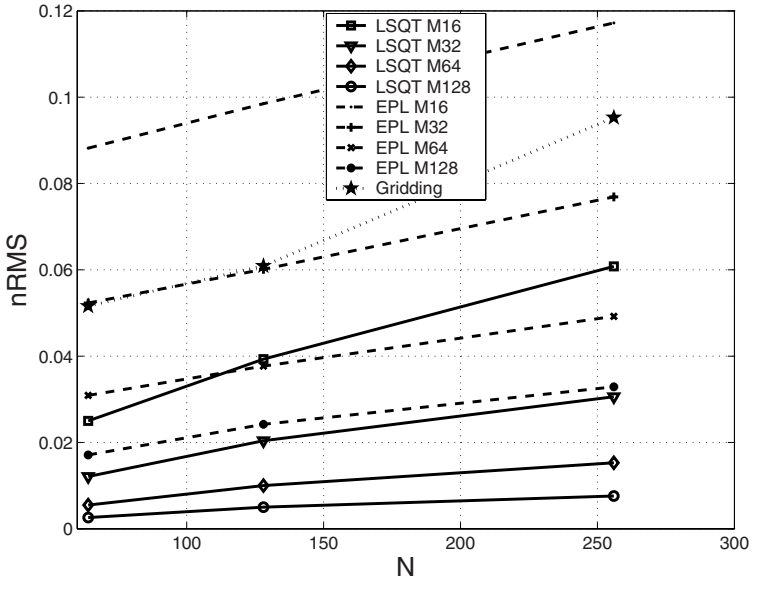

Fig. 2. The nRMS against the size of reconstructed Shepp and Logan phantoms for the LSQT and EPL methods with different M

As we described before, because constructing LSQT is only dependent on the k-space sampling positions and image pixel positions, the LSQT constructed for a given trajectory can be reused for reconstructing the different images with same size. It is affirmative because constructing LSQT is only dependent on the k-space sampling positions and image pixels positions. Moreover, another advantage of LSQT method is that the LSQT constructed in the case of $L < N \times N$ can be reused in the case of $L \approx N \times N$ and $L > N \times N$ where L is fixed. Fig. 3 (a) and (b) show the nRMS and MAD of LSQT method against the number of group for reconstructing different sizes of phantoms with different LSQTs. Here, LSQT256 N64/128 means reconstructing a 64×64 or 128×128

phantom from 13393 k-space data but with a LSQT constructed in the case of reconstructing 256×256 phantom from 13393 k-space data. LSQT64 N64 and LSQT128 N128 mean reconstructing a 64×64 or 128×128 phantom with their own LSQTs. It can be seen that reconstructing 64×64 and 128×128 phantoms with LSQT256 perform better than with their own LSQTs in nRMS and MAD. The reason is that each element of LSQT256 is obtained from 256×256 $\langle C_p \rangle$'s of interval $[0, 1)$ while each element of LSQT64/128 is obtained from 64×64 or 128×128 $\langle C_p \rangle$'s of interval $[0, 1)$. Obviously, the representative values stored in LSQT256 are more precise than those stored in LSQT64/128 when $\langle C_p \rangle$'s have the similar distribution. This advantage means the LSQT method can be reused not only for reconstructing the different images with same size, but for reconstructing the different images of reduced sizes.

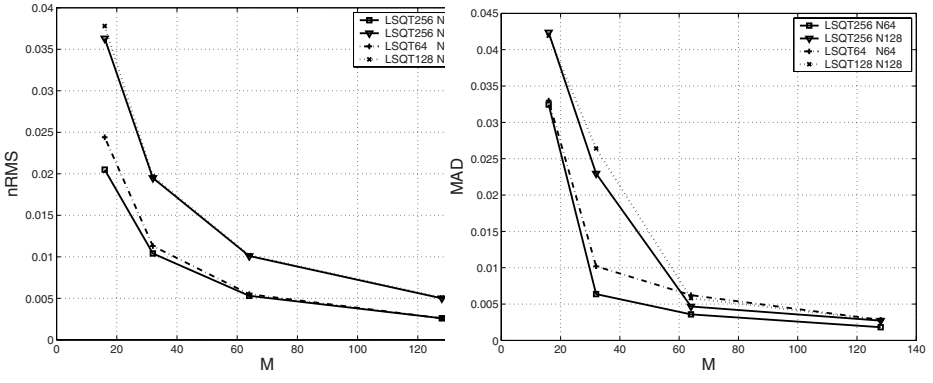

(a) (b)

Fig. 3. (a) and (b) The nRMS and MAD of LSQT method against the number of group for reconstructing different sizes of phantoms with different LSQT's

As we know, the selection of the number of group controls the quantization precision and the size of LSQT and hence the reconstruction accuracy and required memory. Therefore, the selection of M is flexible in trading off required memory against reconstruction error in our method. It means the LSQT method can be customized for the particular application by selecting a predetermined number of groups that corresponds to the desired required memory. For example, if a high accuracy is desired, it is easy to implement by increasing the number of groups. Additionally, the selection of M avoids having the user choose more specific parameters of reconstruction like window width or neighborhood definition like other methods [2,9]. Fig. 4 illustrates the effect of the number of groups on the nRMS and MAD for reconstructing different sizes of Shepp and Logan phantoms when the size of k-space is fixed. The figure suggests that when $L > N \times N$, M can take a small value while when $L < N \times N$, M should take a large value to retain a substantial reduction in reconstruction error.

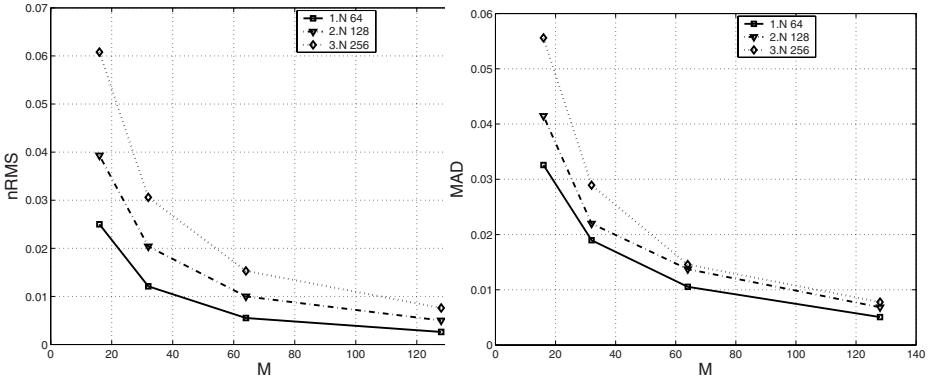

(a) (b)

Fig. 4. (a) and (b) The nRMS and MAD against the number of groups for reconstructing different sizes of Shepp and Logan phantoms when the size of k-space is fixed

4 Conclusion

In this paper, the LSQT method proposed recently by the authors is explored in further detail in its adaptability, reusability and choice of the number of groups. The experimental results show further that LSQT performs better in reconstruction accuracy than EPL and has better adaptability than EPL when facing different reconstruction cases. Moreover, LSQT can be reused for reconstructing different images of reduced size.

Acknowledgments. This work was supported in part by the University Research Committee of the University of Hong Kong under Grant Number URC-10207440.

References

1. Maeda, A., Sano, K., Yokoyama, T.: Reconstruction by Weighted Correlation for MRI with Time-varying Gradients. IEEE Trans. Med. Imag. 7, 26–31 (1988)
2. Jackson, J.I., Meyer, C.H., Nishimura, D.G., Macovski, A.: Selection of a Convolution Function for Fourier Inversion Using Griding. IEEE Trans. Med. Imag. 10, 473–478 (1991)
3. Qian, Y.X., Lin, J.R., Jin, D.Q.: Direct Reconstruction of MR Images From Data Acquired on a Non-Cartesian Grid Using an Equal-Phase-Line Algorithm. Magn. Res. Med. 47, 1228–1233 (2002)
4. Dale, B., Wendt, M., Duerk, J.L.: A Rapid Look-up Table Method for Reconstructing MR Images from Arbitrary K-space Trajectories. IEEE Trans. Med. Imag. 20, 207–216 (2001)
5. Liang, D., Lam, E.Y., Fung, G.S.K.: Direct Reconstruction of Spiral MRI using Least Square Quantization Table. IEEE International Symposium on Biomedical Imaging: From Nano to Macro, 105–108 (2007)

6. Liang, D., Lam, E.Y., Fung, G.S.K.: A least square quantization table method for direct reconstruction of MR images with non-Cartesian trajectory. Journal of Magn. Res. 188, 141–150 (2007)
7. Gersho, A., Gray, R.M.: Vector Quantization and Signal Compression. Kluwer Academic Publishers, Boston (1992)
8. Shepp, L.A., Logan, B.F.: The Fourier Reconstruction of A Head Section. IEEE Trans. Nucl. Sci. NS-21, 21–43 (1974)
9. Rosenfeld, D.: An Optimal and Efficient New Griding Algorithm Using Singular Value Decomposition. Magn. Res. Med. 40, 14–23 (1998)